Mitigation of Dust Impact on Solar Collectors by Water-Free Cleaning With Transparent Electrodynamic Films: Progress and Challenges

Malay K. Mazumder, *Life Fellow, IEEE*, Mark N. Horenstein, *Life Fellow, IEEE*, Nitin R. Joglekar, *Member, IEEE*, Arash Sayyah, Jeremy W. Stark, Annie A. R. Bernard, Sean M. Garner, Julius E. Yellowhair, Hung Yi Lin, Ryan S. Eriksen, Alecia C. Griffin, Yujie Gao, Ricci La Centra, and Alexis H. Lloyd

***Abstract*—Energy-yield loss caused by soiling of photovoltaic modules and concentrated solar power (CSP) mirrors in utility-scale power plants installed in semiarid lands and deserts would result in unsustainable demands for fresh water needed for cleaning. This paper reviews the progress of the electrodynamic screen (EDS) film technology for frequent water-free cleaning with low-energy requirements. Results presented here, based on laboratory-scale EDS-film-laminated solar panel cleaning, show that the output power can be restored higher than 95% of the initial power under clean conditions. For solar mirrors, the specular reflection efficiency can be maintained over 90% ensuring high efficiency of the CSP plants. Operation of the EDS film for maintaining high optical efficiency of solar collectors requires less than 0.2 Wh/m^2/cleaning cycle. Principles, optical modeling, construction, lamination of the EDS films on modules and mirrors, and experimental data showing optical efficiency restoration without water consumption are presented. Current challenges in developing electrodes that would meet optical and conduction properties, low-cost production, and meeting long-term outdoor durability of the EDS films are discussed.**

***Index Terms*—Cleaning, dust impacts, electrodynamic screen (EDS), flexible glass, optical efficiency, solar collectors.**

Manuscript received December 16, 2016; revised May 26, 2017; accepted June 22, 2017. Date of publication July 28, 2017; date of current version August 18, 2017. This work was supported by the Department of Energy (DOE CSP APOLLO EE-0007119) through research project on "Enhancement of Optical Efficiency of CSP Mirrors for Reducing O&M Cost via Near-Continuous Operation of Self-Cleaning Electrodynamic Screens" and cost-sharing grants from Massachusetts Clean Energy Center and EDS Chile SpA. *(Corresponding author: Malay K. Mazumder.)*

M. K. Mazumder, M. N. Horenstein, A. A. R. Bernard, R. S. Eriksen, and A. C. Griffin are with the Department of Electrical and Computer Engineering, Boston University, Boston, MA 02215 USA (e-mail: mazumder@bu.edu; mnh@bu.edu; annieber@bu.edu; reriksen@bu.edu; aleciag@bu.edu).

N. R. Joglekar is with the Questrom School of Business, Boston University, Boston, MA 02215 USA (e-mail: joglekar@bu.edu).

A. Sayyah was with the Department of Electrical and Computer Engineering, Boston University, Boston, MA 02215 USA. He is now with the Department of Chemical Engineering, Massachusetts Institute of Technology, Cambridge, MA 02139 USA (e-mail: arashs@mit.edu).

J. W. Stark was with the Department of Electrical and Computer Engineering, Boston University, Boston, MA 02215 USA. He is now with MagCanica, San Diego, CA 92117 USA (e-mail: jwstark@bu.edu).

Y. Gao, R. La Centra, and A. H. Lloyd are with the Division of Materials Science and Engineering, Boston University, Brookline, MA 02446 USA (e-mail: yujiefly@bu.edu; lacentra@bu.edu; ahlloyd@bu.edu).

S. M. Garner is with the Corning Research and Development Corporation, Corning, NY 14831 USA (e-mail: garnersm@corning.com).

J. E. Yellowhair is with the Concentrating Solar Technologies Department, Sandia National Laboratories, Albuquerque, NM 87185 USA (e-mail: jeyello@sandia.gov).

H. Y. Lin is with the Industrial Technology Research Institute, Hsinchu 31040, Taiwan (e-mail: hylin@itri.org.tw).

Color versions of one or more of the figures in this paper are available online at http://ieeexplore.ieee.org.

Digital Object Identifier 10.1109/JPHOTOV.2017.2721462

I. Introduction

HOT deserts and semiarid areas cover more than one-fourth of the Earth's total landmass; these vast areas receive the highest solar irradiance and least interruptions from cloud and rain. Utility-scale solar plants are mostly installed in semiarid and desert lands and are subjected to high dust deposition rate. Dust layer build-up on solar collectors causes a major energy-yield loss [1]–[5]. For high optical efficiency of solar collectors such as photovoltaic (PV) modules and concentrating mirrors, the optical surface must be kept clean against dust deposition that reduces the efficiency of light transmission. To maintain optical efficiency of solar collectors close to its initial value under clean condition, frequent cleaning is needed at intervals depending upon the rate of dust deposition at the plant site.

Washing solar collectors with water and detergent is the most commonly practiced method for cleaning [6]–[9]. The conventional approach for cleaning collectors in utility-scale plants is to use a large truck with a water tank and a pump system for spraying deionized water. Robotic brush cleaning is also used for smaller solar plants, which uses less water and detergent [10]–[13]. However, manual or robotic cleaning with water is often a critical problem in areas where water is scarce and conservation of water is needed. In addition, these methods are both labor and energy intensive and are interruptive to routine plant operations. If the global solar power output is to increase to hundreds of gigawatt levels, as is envisioned, efficient operation of solar plants would result in an unsustainable demand for fresh water. Unless a water-free or a low-water cleaning method is established, continued growth in global utilization of solar power plants may lose public support in areas suffering long intervals of drought.

One of the promising low-water-based cleaning processes is to apply a transparent superhydrophobic (SH) coating with nanostructured surface on the optical collectors for reducing adhesion of dust particles to improve cleaning efficiency with

low water use [14], [15]. This is a passive method used for modifying the surface properties of solar collectors to make them easily cleanable. Of the three adhesion forces between deposited dust particles and the surface of the collectors, SH surface treatment reduces both capillary force and van der Waals force but does not significantly affect the electrostatics image force of adhesion. Current SH coatings reduce adhesion forces but do not provide any dust removal force; water is still needed for cleaning. Outdoor lifetime of the SH surface treatment is limited to a few months unless the surface is frequently cleaned. SH coating application in a large scale has not been established yet. Interestingly, SH coating would work the best where rainfall is frequent or wind speed is high enough to remove loosely bound dust.

Application of transparent electrodynamic screens (EDS) [16]–[22] is an emerging method for cleaning solar collectors by the electrostatic removal of the deposited dust layer. The method can be used for cleaning solar modules, parabolic troughs, and heliostats. Studies to date show feasibility of EDS film integration on or retrofitting the optical surfaces of solar collectors after installation for maintaining high transmission or reflection efficiency without requiring water. EDS is an active method that applies electrostatic force to lift dust particles and expel them from the surface of the solar collectors when activated. The energy requirement for EDS operation is an infinitesimal fraction of the energy derived from the solar collectors and can remove more than 90% of the dust deposited on the surface in less than 2 min when EDS is activated. Being an electrodynamic dust removal process, the EDS film is designed primarily for removal of dust from solar collectors; its application in large-scale solar plants located in semiarid and desert areas would provide significantly increased energy yield by frequent cleaning where the atmosphere is often dry and dusty with very low rainfall. The atmospheric conditions in these areas vary over wide ranges of temperature and relative humidity (RH). EDS film application needs to meet the requirements of temperature and RH cycling, UV radiation resistance, and dust impact resistance under dust storms. As an example, in early morning hours, the temperature dips and RH becomes high reaching the dew point, particularly in areas close to an oceanfront. Thus, the deposited dust often goes through these temperature and RH cycles.

This paper presents a brief description of the principles of operation of the EDS film for removing dust from the surface of solar collectors, design, and lamination of the EDS film on the optical surface of PV modules and solar mirrors. We summarize the progress made to date and the potential of the EDS film technology for mitigating dust impact on solar collectors with water-free cleaning and the current technical challenges for its high efficiency and durability. The EDS film would provide an effective dust shield against desert dust, but occasional water-based cleaning would still be required for removing atmospheric pollutants such as soot arising from automobile exhausts, particle-bound sulfates and phosphates that often deposit forming organic films, and sticky contaminates like birds droppings. The frequency of water cleaning with detergents and brushing would be greatly reduced along with the associated consumption of water. We reported a cost model [23], which is currently under further development based on the EDS film production, lamination, and operation along with occasional water-based cleaning. This model encompassing a comprehensive cleaning process for solar collectors using the EDS film and occasional water-based washing with an estimated cost saving and water conservation is currently under progress, waiting for the completion of the field testing.

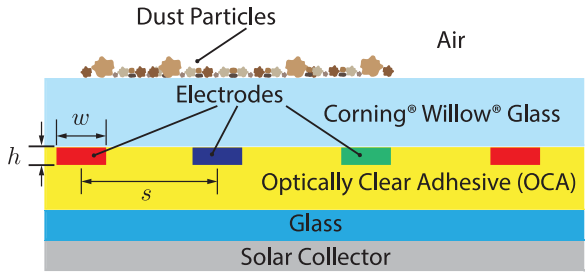

Fig. 1. EDS film lamination on a solar mirror or front glass plate of a PV module. The top layer is composed of a flexible glass (100 μm in thickness) facing the solar radiation with its backside printed with parallel electrodes affixed with the front surface of the solar collectors with an OCA film. The solar collector represents a PV module or a mirror surface in a CSP system.

II. Electrodynamic Screen

An EDS film consists of rows of interdigitated parallel electrodes embedded within two transparent dielectric films, as shown in Fig. 1. The film at the top with the sun-facing front side is made of transparent ultrathin flexible glass (Corning® Willow® Glass for example) [24], which serves as a superstrate for depositing transparent (or reflective) conducting electrodes. The electrodes are encapsulated by using a transparent pressure-sensitive optically clear adhesive (OCA) film [25]. The backside of the OCA film has a release liner; the release liner is removed for laminating the EDS film on a solar collector surface. Once the release liner is taken out, the EDS film can be used for retrofitting on the front cover-glass plates of the solar panels or on the concentrating solar mirrors. Reflective conductive electrodes are used only for solar mirrors, while transparent conductive electrodes can be used both for solar panels and mirrors. Beside the EDS film, a three-phase power supply unit is needed to activate the electrodes.

Except for the electrodes, the light transmission efficiency of the glass film and the OCA films is higher than 99% when corrected for reflection losses. The indices of refraction of the flexible glass and the OCA film match closely to the glass cover plates of the PV modules or second surface glass mirrors. The pressure-sensitive OCA films used for lamination of the EDS film that meet solar field operation requirements with respect to temperature and RH cycling under solar UV radiation exposure are commercially available [25]. These acrylic-based OCA film would be sandwiched between the Willow® Glass and the front glass cover plates of the solar collectors. The prototype EDS films with the OCA have been tested in the laboratory for their UV radiation resistance and pulsed high-voltage (1.5 kV) operation without any observable degradation of their performance or optical transparency. The OCA film has been exposed to outdoor

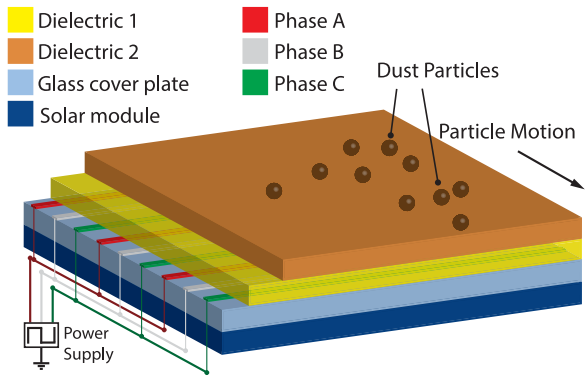

Fig. 2. Schematic representation of a 3-D view of an EDS composed of parallel electrodes for the three-phase pulsed voltage drive [27].

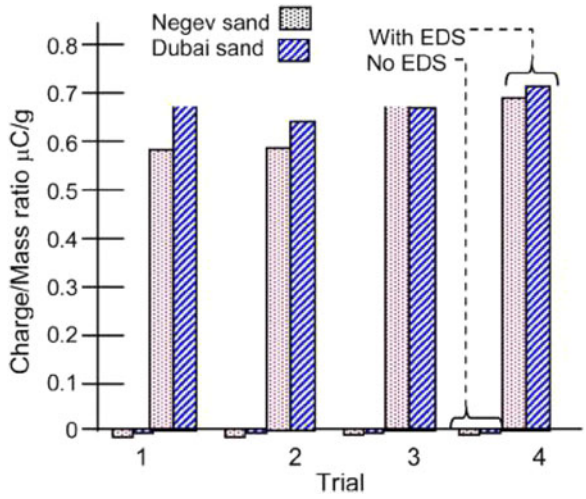

Fig. 3. Charge-to-mass (Q/M) ratio of desert dust particles measured before and after EDS activation show that particles are charged with a high Q/M when EDS is activated [30].

conditions, which included a range of ambient RH and temperatures. The EDS showed no noticeable degradation as a result of these fluctuations. Silicone and EVA-based adhesives are also possible candidates for EDS film lamination if acrylic-based adhesives do not meet the long-term field requirements.

Fig. 2 shows a layout of the parallel electrodes embedded under the flexible glass and a schematic view of particle trajectory over the EDS surface. The electrodes are activated by three-phase high-voltage (1–1.5 kV), low-current (microamp level), and low-frequency (5–20 Hz) pulses. The applied voltage pulses create a time and spatially variant electric field on the EDS surface that charges the dust particles on the surface with positive electrostatic charge. Our studies on the electrostatic charging of the dust particles on the surface of EDS film, with the electrodes activated by the three-phase electric field, show that several processes may simultaneously contribute to the electrostatic charging of the particles including contact charging, tribocharging, corona charging, and the injection of positive charge carriers to the EDS surface from the positive electrodes undergoing microfilamentary discharge (MFD). The experimental results show that the MFD process provides consistent charging of the particles with positive polarity that dominates other charging processes. The positively charged particles are lifted up by the Coulomb force and undergo unidirectional translational motion by the traveling electric field that sweeps the dust particles from the EDS surface [26]. In most of the cases, the charge-to-mass ratio of the dust particles, removed by the EDS action and as measured by using a Faraday cup, are highly charged with positive polarity, regardless of the source of the dust particles. The dust samples collected from different solar fields were used for testing the EDS film.

Efficient electrostatic charging of the particles plays a critical role in EDS-based dust removal. Laboratory experiments were carried out by depositing a standard JSC-1A test dust [28] to examine EDS operation. To examine electrostatic charging characteristics, we used a Faraday cup (Monroe Electronics) [29] for measuring the charge-to-mass ratio of the dust expelled by the EDS activation. Fig. 3 shows the experimental data on the charge-to-mass ratio (Q/M) of dust particles removed by the EDS action after depositing the desert dust particles on an EDS-film-laminated solar panel. The Coulomb repulsion force applied to a particle with a charge q is $q\mathbf{E}$, where $\mathbf{E}$ is the electric field experienced by the particle on the surface of the EDS film when the electrodes are activated. All dust samples were first baked in an oven at 200 °C for 2 h to remove organic materials. The samples were then sieved to remove dust particles with diameter larger than 88 μm. The measured value of Q/M (see Fig. 3) shows near saturation charge. Saturation charge (Gaussian limit [29]) depends mainly upon the surface area, proportional to d_p^2 for spherical particles, in which d_p is the particle diameter. The dust samples tested were in the size of 1–88 μm in diameter. In air, saturation charge limit for an isolated particle is given by 26.4 μC/m^2, which is independent of the dielectric constant of the particles [29]. Therefore, Q/M values of the dust samples were nearly identical, which are close to their saturation charge limit with positive polarity.

Fig. 4(a) shows the cross-sectional schematic of an EDS confuguration, and Fig. 4(b) illustrates the distribution of electrical field vector $\mathbf{E}$ at a given instant of the applied electric field [31]. For an efficient cleaning, the Coulomb force F_{C} [see Fig. 4(c)] must exceed the sum of all forces of adhesion between the particles and the EDS surface $\sum F_{\mathrm{adh}}$, where $\sum F_{\mathrm{adh}}$ represents the summation of all adhesion forces including van der Waals F_{vdW}, capillary F_{cap}, gravitational F_{g}, and electrostatic image force F_{i} [32]. The capillary force of attraction is neglected, since the EDS operation is performed at a low RH ($<$50%). For any charged particle on the surface at a low RH, the major force of adhesion is the electrostatic image force, which is proportional to q^2/t^2, where t is the thickness of the ultrathin glass. The force of removal is the Coulomb force of repulsion is $q\mathbf{E}$; thus, an electric field intensity $\mathbf{E}$ must be high enough to repel the particle [33]. The field $\mathbf{E}$ has two components: one perpendicular to the EDS film surface and the other is parallel to the surface. Three-phase activation of the electrodes, as discussed before, creates a traveling electric field, which helps removing the dust layer in a sweeping motion.

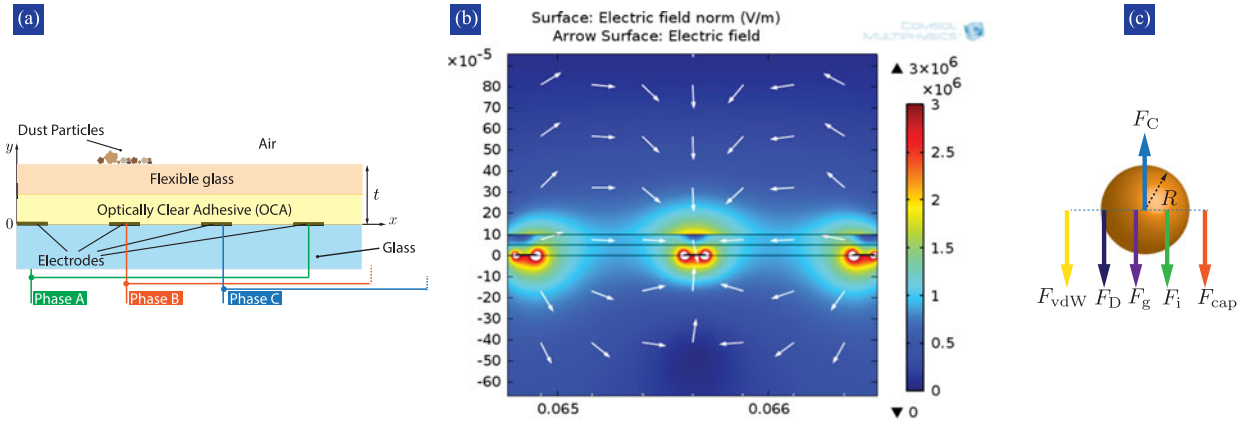

Fig. 4. (a) Cross section of the EDS configuration with two stacked layers of transparent dielectric films and accumulation of dust particles on top of the EDS surface. (b) Electric field norm $|\mathbf{E}|$ and electric vector field (unit: V/m), when the voltages of phases A, B, and C are 1 kV, 0 V, and 1 kV, respectively [31]. (c) Free-body diagram of the forces in the y-direction exerted on the particle sitting on an EDS surface. The terms F_D, F_g, F_i, F_{cap}, F_{vdW}, and F_C denote the vertical components of the dielectrophoretic (DEP) force, gravitational force, image force, capillary force, van der Waals force, and vertical component of the Coulomb force, respectively [32].

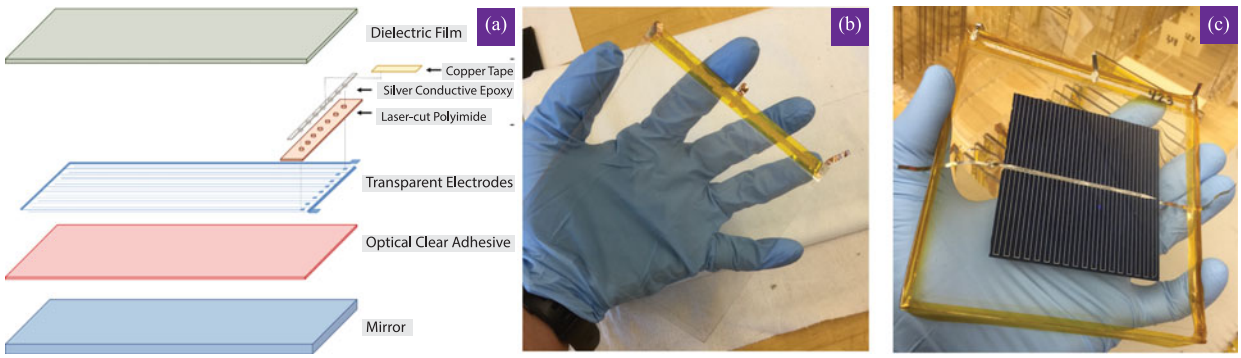

Fig. 5. (a) Construction of a transparent EDS film stack. The top dielectric film is made of ultrathin flexible glass, with the backside printed with transparent conducting electrodes, made of silver nanowire (AgNW), and the electrodes are laminated by an OCA film. The EDS stack is then affixed on a solar mirror (as shown) or a PV module surface. The right strips shows interconnections of the three-phase electrodes. (b) Photograph of an EDS film before lamination on a solar panel. The EDS film was constructed with silver nanowire AgNW electrodes printed on an 100-μm-thick flexible glass (Corning® Willow® Glass). (c) EDS film laminated on a solar panel, the bus bar in the middle is for measuring short-circuit current (I_{sc}) of the solar panel under different conditions.

III. EDS Design and Construction

A. EDS Film Stack Construction

Laboratory-scale (11 cm × 11 cm) EDS film stacks are made by screen-printing electrodes onto the flexible glass and laminating the electrode side of the ultrathin glass on to a solar panel or a solar mirror using an OCA film. The three-phase electrical connections to the electrodes are performed manually using a conductive silver epoxy or by screen-printing with crossover connection. Fig. 5(a) shows the construction of the EDS film stack for lamination on a solar mirror or on a solar panel. Fig. 5(b) shows an EDS film before lamination. The film is flexible and its transparency depends upon the optical properties of the electrodes and geometry of the electrode pattern. Fig. 5(c) shows a solar panel laminated with an EDS film. During the lamination of the EDS film stack, it is necessary to minimize adsorbed moisture on the surface before lamination, which minimizes corrosion of the electrodes and electromigration of silver (Ag) ions if Ag-based electrodes are used. Application of a transparent conductive layer of SnO_2:F or indium tin oxide (ITO) around the silver nanowire (AgNW) electrode may provide a barrier against corrosion caused by moisture and oxygen ingress [34].

B. Lamination of the Flexible EDS Films

Corning® Willow® Glass is manufactured in 1.3-m widths and wound onto spools in 300-m lengths. Commercial production of the EDS for lamination on heliostats would likely consist of four EDS film segments of equal size combined into an array to cover a single heliostat, as shown in Fig. 6. Due to the mechanical properties of Willow Glass, the EDS film can be laminated onto flat or parabolic troughs using similar arrays of EDS for convenient lamination in a solar fields.

C. Scale-Up and Industrial Production of Prototype EDS Films

Fabrication of the EDS film for large-scale production is being evaluated by gravure offset printing (GOP). Currently, we are using Ag-paste electrodes on flexible Willow Glass. The printing

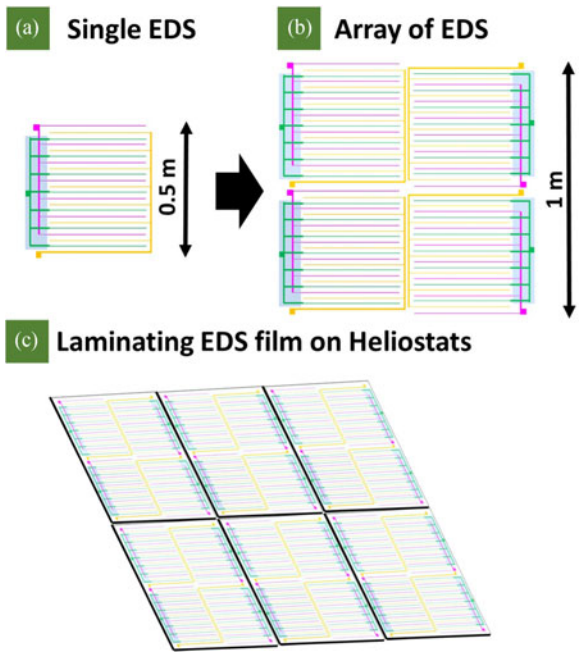

Fig. 6. (a) EDS film (0.5 m × 0.5 m), (b) an array of four EDS films to cover solar mirror (1 m × 1 m), and (c) laminating EDS films on flat or curved surface of solar collectors.

process is applicable for roll-to-roll production in larger sizes. Compared with screen-printing, GOP provides better precision of the geometric pattern of electrodes. Ag-paste electrodes are currently used for their proven long-term durability in their applications to PV modules using monocrystalline silicon solar cells. A GOP printing facility is used to produce a small-size prototype EDS film (12 cm × 12 cm) for evaluation under different environmental conditions, simulating solar fields.

D. Optical, Electrical, and Mechanical Properties of the EDS Film

Both ultrathin flexible glass and the OCA film used for the EDS film meet the required low-light transmission loss (<0.5%) over the entire solar radiation spectrum, when corrected for the reflection loss. These materials are insulators, flexible, and meet the requirement of UV radiation resistance and outdoor durability. The flexible glass also provides dust impact resistance against erosion. For successful operation of the EDS film, the most critical aspect is the choice of electrode material for 1) high transparency ($T > 85\%$) for PV modules or high specular reflectance (SR) (>85%) for CSP mirrors, 2) low sheet resistance, denoted as R_s (preferably $R_s < 200\ \Omega/\square$), 3) mechanical flexibility, 4) low-cost roll-to-roll production in a large scale, and 5) outdoor durability (25+ years). None of the available electrode materials meets all of the requirements. For example, Ag-paste electrodes provide proven durability in solar fields as used in monocrystalline silicon solar panels, but they are opaque and cause shading loss. Silver nanowire (AgNW) has both high transparency and high conductivity, but its outdoor durability has not been established.

Our previous studies using AgNW electrodes [35] showed that it is possible to reach dust removal efficiency (DRE) > 90%, SR > 90%, and specular reflectivity restoration (SRR) > 95%; it was found that AgNW electrodes, as used in the EDS film, have poor durability. One of the major challenges in EDS film applications is the outdoor durability of conducing transparent or reflective electrode materials. Oxidation and corrosion of AgNW electrodes are caused by moisture and oxygen ingress and by silver ion migration that degrade the silver-based electrodes outdoors. Recent studies show that if AgNW electrodes are encapsulated by a protective coating, its durability is improved substantially [34], [36]. No field data on its durability have been presented yet.

IV. Modeling of the Optical Properties of the EDS Film

A. Electrode Materials and Geometrical Pattern

The choice of material for the electrodes is determined by the required optical and electrical properties and by the need for high-volume low-cost production. To meet several requirements for electrode deposition on flexible glass, we are limiting our choice to 1) AgNW for its high transparency and low sheet resistance, 2) silver ink (silver nanoparticles) as reflective electrodes on the EDS film for their applications to the second surface silver mirrors, and 3) carbon nanotubes for their applications to both PV modules and CSP mirrors. Applications of ITO, graphene, or other materials that need either chemical vapor deposition or photolithography for patterning the electrodes were considered, but the added cost in EDS film production is of concern. AgNW provides the best performance as an electrode material because of its unmatched electrical and optical properties, but its durability is poor unless a protective layer is applied to minimize degradation [34]. Recent advancements of electrode materials needed for touch screens are likely to provide additional choices for electrode materials and on the method of encapsulation of AgNW.

B. Optical Transmission Losses Caused by EDS Film Lamination

Transmission loss of sunlight by EDS lamination needs to be minimum for its efficient operation. The transmission loss of the EDS films depends both upon the optical properties and the geometrical pattern of the electrodes. The FRED Optical model [37] was used for two electrode geometries and for electrode materials with different optical transparency, as shown in Table I. The two geometries listed in Table I refer to Fig. 1, defining w, h, and s. Optical loss caused by the ultrathin glass and the OCA film was considered negligible. The model showed the calculated transmission efficiency after 4% loss caused by front surface reflection by the glass surface at normal incidence. This reflection loss is always present with or without the EDS film unless the glass surface is coated with an antireflective coating. We assume that the Ag-paste electrode will be opaque with 0% transmission as shown in row 1 and AgNW electrodes will have 95% transmittance as shown in row 6 of Table I. It is desired to

TABLE I
FRED OPTICAL MODELING OF SUNLIGHT TRANSMISSION EFFICIENCY OF THE EDS-FILM-LAMINATED SOLAR PANEL AFTER 4% FRONT-SURFACE REFLECTION LOSS

Optical Transmittance by EDS Electrodes T	Transmission After EDS Lamination	
	Geometry 1 $w = 30\ \mu$m, $h = 3.5\ \mu$m, $s = 500\ \mu$m	Geometry 2 $w = 80\ \mu$m, $h = 0.95\ \mu$m, $s = 700\ \mu$m
0.0	0.90	0.85
0.6	0.93	0.91
0.8	0.94	0.93
0.85	0.95	0.94
0.9	0.95	0.95
0.95	0.95	0.95

minimize transmission loss caused by the EDS film lamination below 1.5%; therefore, this loss becomes only a small fraction of the optical efficiency regained by the self-cleaning action of the EDS film and the corresponding increase of energy yield.

The column at the left in Table I shows optical transmittance of the electrode and corresponding values of the EDS film transmission efficiency given in the right column. For an electrode with light transmission (T) efficiency of 80%, we assumed that the loss involves both absorption and scattering losses.

For electrode geometry 1, as shown in Table I, the transmission efficiency of the overall EDS films are tabulated for different values of the electrode transmission efficiencies. It is necessary to have the electrodes with at least 80% transmittance (T) to have the EDS film transmittance 94.53%. Thus, the overall transmission efficiency of 94.53% of the EDS film with 4% front surface reflection loss shows that EDS film lamination is causing only 1.47% loss with electrodes having 80% transmittance. This requirement can be met with ITO and AgNW electrodes. For electrode geometry 2, with wider electrodes compared with geometry 1, it is necessary to have the electrodes with at least 85% transmittance to have the EDS film transmittance 94.07%. Table I shows that the electrodes must have high transmittance over the range of wavelength covered by the solar panels. To achieve high transmittance T and high conductivity or a low R_s, preferably less than 200 $\Omega/\square$, there is always a tradeoff between transparency and electrical conductivity of all electrode materials considered here.

In these modeling calculations, we have not considered the fact that a portion of the forward scattered light from the electrodes will enter the solar panel at oblique angles, which would provide a larger optical path length in the absorption medium and thus higher collection efficiency compared with the model calculation. For solar mirrors, particularly for heliostats, both absorption and scattering losses affect the reflection efficiency.

C. EDS Electrode Design for High Reflection Efficiency of Solar Mirrors

For designing the EDS film for solar mirrors, the goal is to have a high SR. The high SR of the EDS film can be achieved using either transparent conductive electrodes or reflective conducting electrodes. To achieve reflective conductive electrodes, there is no stringent tradeoff between the electrical conductance of the electrodes and its surface reflectivity. In this case, the electrodes can be of any conductive material with reflective surface properties. Since silvered mirrors are used in CSP application, electroplated silver electrodes that provide high reflectivity on both front and backsides could provide the reflectance over the entire solar spectrum needed for CSP applications, as shown in Fig. 7. Fig. 7 shows ray optics of an EDS film with reflecting conductive electrodes with flat surfaces. The major technical challenge is to print electrodes, rectangular in shape, with smooth front and back surface coated with silver to provide high specular reflectivity. The GOP process is compatible for applying reflective coatings on both front and backsides of the electrodes.

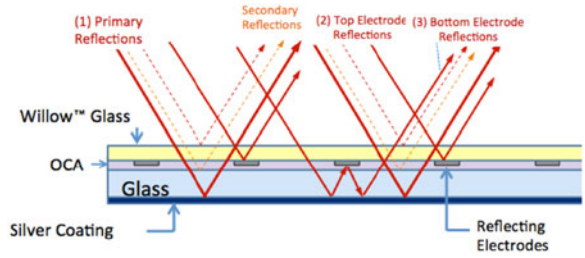

Fig. 7. Schematic representation of an EDS film with reflective electrodes laminated on a solar mirror.

D. Reflection Losses in EDS Film-Laminated Solar Mirrors

Reflected rays from both front and backsides of electrodes of the EDS film are considered to model the overall SR efficiency for a given electrode geometry, as shown in Fig. 7. Table II shows the SR efficiency of an EDS film-laminated solar mirror. The two listed geometries in Table II refer to Fig. 1, defining w, h, and s. The model assumes that the solar mirror has 100% specular reflectivity and calculates the SR efficiency after EDS lamination with rectangular electrodes of different reflectivity of front and back surfaces. The leftmost column shows the front surface reflectivity, denoted as $R_{\rm FS}$, varying from 0% to 95% and back surface reflectivity, denoted as $R_{\rm BS}$, either having the same reflectivity (second column) as the front side or nonreflecting (third column). For example, if the front electrode surface is silver-plated to have 60% reflectivity and the backside of the electrodes is completely absorbing without reflective coating (similar to that of Ag-paste electrodes), the optical model predicts that the overall SR of the EDS-laminated mirror would be 82%. FRED Optical modeling of reflecting electrodes can be determined from Table II for an angle of incidence 15°. The table shows that if the electrodes have reflection efficiency 90% or higher for both sides, the SR loss would be less than 3%.

We are currently using silver ink electrodes, commercially available from Henkel Electronics ECI 1011 [38], for producing the EDS film for CSP mirrors. This electrode material is similar to Ag-paste electrode but has high diffused reflectance because of the surface roughness of the printed electrodes. This electrode material is considered to have similar outdoor stability as that

TABLE II
FRED OPTICAL MODELING OF SPECULAR REFLECTIVITY OF THE EDS FILM WITH REFLECTIVE ELECTRODES WITH DIFFERENT REFLECTIVITIES FOR TWO ELECTRODE GEOMETRIES

Reflectivity of Front Surface of the Electrodes	Specular Reflection After EDS Film Lamination			
	Geometry 1 $w = 42.5\ \mu$m, $h = 3.5\ \mu$m, $s = 500\ \mu$m		Geometry 2 $w = 80\ \mu$m, $h = 0.95\ \mu$m, $s = 700\ \mu$m	
R_{FS}	$R_{BS} = R_{FS}$	$R_{BS} = 0$	$R_{BS} = R_{FS}$	$R_{BS} = 0$
0	—	0.82	—	0.81
0.6	0.92	0.87	0.91	0.88
0.7	0.94	0.88	0.93	0.89
0.8	0.95	0.89	0.95	0.90
0.9	0.97	0.90	0.97	0.91
0.95	0.98	0.90	0.98	0.92

of the Ag-paste electrodes [38]. One of the challenging tasks is to make the surface secularly reflective by silver plating.

V. EXPERIMENTAL STUDIES, RESULTS, AND DISCUSSION

A. Measurements of Dust Removal Efficiency, Output Power Restoration, and Specular Reflectivity Restoration

Experimental studies were performed to measure DRE, output power restoration (OPR) of EDS-film-laminated solar panels, and SRR of EDS-film-laminated solar mirrors. An environmentally controlled test chamber was used for evaluation of all laboratory-scale EDS films. A sieve (no. 170) with nominal openings of 88 μm was used to classify test dust particle to have an upper cutoff diameter $d_p < 88\ \mu$m, where d_p denotes the particle diameter. As a test dust, we have used JSC-1A dust [28] to simulate atmospheric particles in desert climate. This test dust compositions are, approximately, as follows: SiO_2 (47%), Al_2O_3 (16%), CaO (10%), MgO (10%), FeO (8%), Fe_2O_3 (3%), Na_2O (3%), and TiO_2 (2%). To verify our experimental data against wind-blown dust of a solar field, we used dust samples collected from the Sandia National Laboratories' solar field. Test dust was deposited on the EDS-film-laminated solar panels or solar mirrors placed under the sieve and manually shaken to obtain a surface mass concentration of dust at a desired level ranging from 1 to 30 g/m^2. Most of the experiments were performed with surface mass density from 1 to 5 g/m^2. The details of the experimental procedures were reported earlier [20], [21], [39], [40].

The DRE was measured by the gravimetric method from the ratio of $(m_0 - m_r)/m_0$, where m_0 is the dust mass deposited on the EDS film (surface area approximately 100 cm^2), and m_r is the dust mass remaining on the film after EDS activation.

The OPR was determined by measuring the short-circuit current, denoted as I_{sc}, under three conditions:

1) with clean EDS solar panel I_{sc};
2) the loss of I_{sc} (ΔI_{sc}) after dust deposition;
3) the restored I_{sc} after activating the EDS for 1 min.

Since the open-circuit voltage (V_{oc}) and the fill factor remain practically constant for a given irradiance and wavelength (550 nm) of radiation, the ratio (restored I_{sc})/(initial I_{sc}) provides the fractional output power restored. Similarly, SRR was determined by the ratio (restored SR)/(initial SR). The experimental arrangements for measuring OPR and SRR are shown in Fig. 8.

Twenty-two EDS films were produced and evaluated for DRE, OPR, and SRR. Results of only ten samples, of no particular order, are presented in Fig. 9. The average DRE for all 22 EDS films was 88.1% with standard deviation $\sigma = 4.9$. The mean OPR for all samples was 95.5% with $\sigma = 1.80$. The mean SRR value was 88.9% with $\sigma = 2.15$. SRR values were low, since the reflectivity of the electrode surface was only about 20%. Each experiment was conducted ten times, and the result shown is the average of ten readings. Both OPR and SRR depend upon the DRE of the EDS film. Fig. 9 shows that the output power of a solar panel is far less sensitive on the dust mass concentration on the EDS film surface compared with SRR of the solar mirrors. Light reflected by the mirror to the receiver travels twice through the dust layer, and only specularly reflected light can reach the receiver.

B. Effects of Relative Humidity and Temperature Variations

In most of the solar fields in desert areas, there would be wide variation in RH and temperature. Since the dust deposition continues throughout the day, the deposited dust layer will undergo RH and temperature variations. At a high RH, the moisture layer around the dust particles will increase capillary adhesion between the dust layer and the EDS film surface and between individual particles. The objective here is to examine if the DRE of an EDS film changes after the deposited dust layer went through a RH cycling. Table III shows the experimental data on DRE by 1) depositing a dust layer on the film at a low RH and then activating the EDS, and 2) depositing a dust layer and exposing it for a couple of hours at a high RH and then measuring the DRE at RH less than 50%. The results show that there was no reduction of DRE; the DRE was slightly improved possibly because some fine particles were agglomerated with large particles and got removed.

In hot desert environments, the solar panel may operate at ambient temperatures close to 40 °C, while the cell temperature may reach 60 °C. Thus, it is necessary to operate EDS in a wide range of temperatures. At high-altitude areas, temperature may

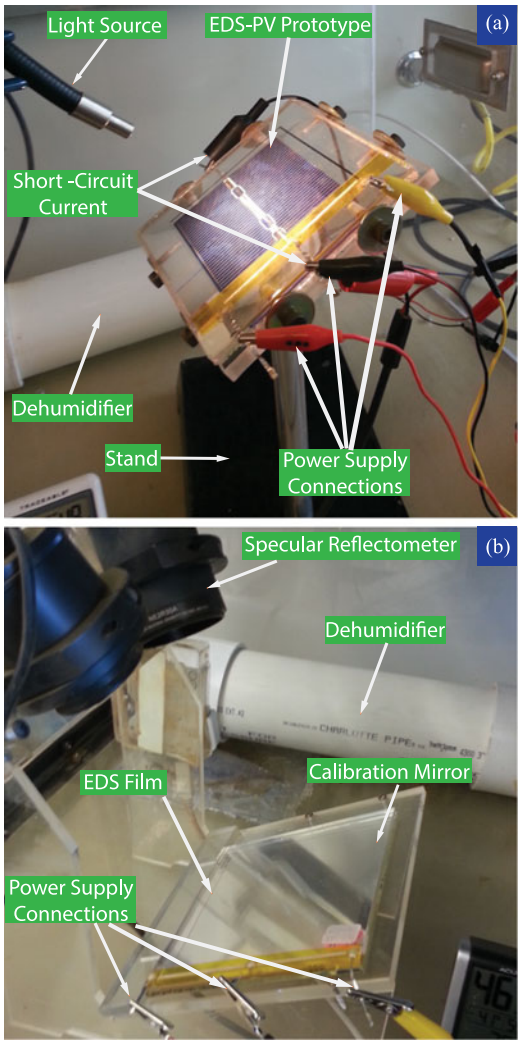

Fig. 8. Photographs showing the experimental arrangements for measuring (a) OPR and (b) SRR. (a) EDS film laminated solar panels is positioned at a desired tilt angle and placed in a climate-controlled test chamber for measuring short-circuit current under different conditions. (b) Noncontact specular reflectometer is used to measure specular reflection of a solar mirror laminated with an EDS film.

dip down below 0 °C. At a high irradiance, the solar panel operates at a temperature of 20 °C above the ambient temperature; it is anticipated that the EDS film would be exposed to temperatures ranging from below 0 °C to 60 °C or higher and RH varying from 20% to 90% or higher. The expansion of the EDS film stack at high temperature and contraction at low temperature could cause a major mechanical stress. The encapsulation must withstand the temperature and RH variations.

C. Energy Consumption

Power requirement and energy consumption of EDS were measured at 20%, 30%, 40%, 50%, and 60% RH to estimate the energy consumption per m^2 of the EDS film. The energy consumption by the EDS film was determined by measuring current drawn by the EDS film and the pulsed high voltage power supply, operating with 1.2 kV, three phases, and

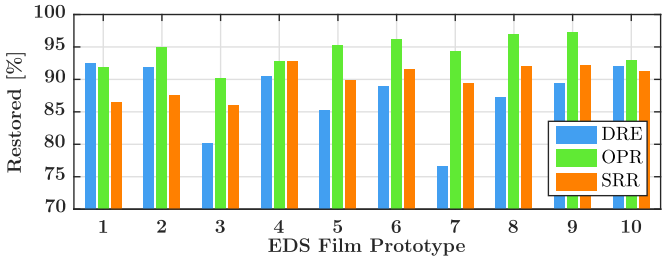

Fig. 9. DRE, OPR, and SRR for different EDS films measured in the range of RH (30–50%), temperature (20–25 °C), with a tilt angle of 30°.

5 Hz. Table IV shows the measured values of the current drawn from the 12-V dc power supply by two EDS films without activation and with activation. The results show that energy requirement per m^2 of the EDS film, when activated, would be less than 0.2 Wh/m^2/cleaning cycle. The measured values of energy consumption show that energy requirement for the EDS power supply is approximately 0.003% of the energy produced by a solar panel operating in a semiarid or desert area, if dust cleaning is performed once a week. It is estimated that each cleaning cycle would require a maximum operational time of 100 s. The EDS electrodes operate under a capacitive load between the electrodes encapsulated by dielectric material. The estimated value of the interelectrode capacitance is in the range of 150–200 pF and interelectrode resistance is of the order of 20 MΩ for an EDS with a surface area 100 cm^2. The frequency of operation is in the range of 5–10 Hz. Thus, the impedance of the EDS film is very high.

On the surface of the EDS film, the electrostatics dust removal force is directly applied to the particles. Theoretical calculation on the minimum energy requirement for removing a dust layer with a surface mass density 30 g/m^2, which is the average annual dust deposition rate in the Mojave Desert, is less than 0.02% of the energy derived from the solar panels of the same area per day.

D. EDS Film Applications in Different Solar Fields

While EDS technology provides a water-free dust removal method, it has many limitations. The method is applicable to desert sand for their removal from the EDS surface under relatively dry condition at RH below 50%. When the dust particles are very cohesive, because of their high surface energy (often measured by their angle of repose), capillary force becomes significant. An example is the case of so-called mud rain; in some places of the Middle East, a drizzling rain associated with dust storm creates formation a very cohesive dust layer on the solar collectors surface. When the mud dries up, it adheres to the solar collector surface very strongly, requiring brush cleanings with water and detergent. Occasional water cleaning may be needed in solar fields to remove highly adhesive pollutants such as soot, organic films, and bird droppings.

VI. Cost Analysis

A cost analysis is needed for cleaning solar collectors in fields under different climates for possible lowering of the oper-

TABLE III
DRE PERFORMANCE OF AN EDS FILM BEFORE AND AFTER RH CYCLING

Experiment #	Initial Mass Density of Dust [g/m^2]	RH of Dust Deposition [%]	Max. RH of Dust Layer Exposure [%]	RH of EDS Film Operation [%]	Measured DRE [%]
Initial	5.20	28	28	28	90.48
1	5.52	30	80	46	93.26
2	4.89	30	80	48	92.86
3	5.10	30	80	47	94.06
4	5.04	30	80	45	94.92
5	5.53	30	80	41	93.81
Ave. (1 to 5)	5.22				93.70

TABLE IV
ENERGY CONSUMPTION PER AREA OF THE EDS FILM PER UNIT CLEANING CYCLE

RH (%)	Current Drawn, no EDS (mA)	Current Drawn, Two EDS Films (mA)	DC Power (mW)	Surface Power Density (W/m^2)	Energy (Wh/m^2/cycle)
20	54.64	68.13	161.88	11.33	0.189
30	54.66	68.03	160.44	11.24	0.187
40	54.62	68.1	161.76	11.33	0.189
50	54.65	68.2	162.6	11.39	0.189
60	54.65	67.9	159	11.13	0.186

The results presented are based on using two EDS films.

ation and maintenance (O&M) cost by EDS film installation and operation with occasional water-based cleaning. Experimental data on the evaluation of the EDS film samples are needed in large-scale solar plants for frequent removal dust and achieving a high performance ratio (PR) of the plant by maintaining high optical efficiency. The PR is the ratio of actual energy yield for a solar plant to the designed capacity of energy yield for the plant over a period of one year. Once an EDS manufacturing process for low-cost production is established, it would be possible to optimize EDS film operation with occasional water-based cleanings for lowering O&M cost, enhancing annual energy yield.

Removal of deposited dust by deploying an EDS-based cleaning system provides benefits not only in terms of savings in the variable cost, such as the annual water consumption, but also as reduced fixed cost in terms of the size of the power plant (e.g., number of CSP mirrors or PV modules needed to deliver a fixed amount of power). A portion of these benefits is offset by the cost of the producing, installing, and operating the EDS film. A comparative study between three different cleaning methods, including SH coating, pressurized air cleaning, and EDS film application, has been reported recently [41]. These costs and benefits are captured in terms of the levelized cost of operating the EDS system using a cost modeling method outlined in [23]. The calculated cost per m^2 for the EDS film is based on printing the silver ink electrodes on flexible glass using the GOP process. A detailed cost model is currently under development. In this model, a 0.35 technology improvement multiplier is applied owing to learning effects incorporated within the cost analysis model. The calculated levelized cost of mirror cleaning (LCOMC) has a mean of \$0.0056/kWh with a standard deviation of \$0.0003/kWh for a million units of production annually. Our cleaning schedule assumes that this system will only use water only when it is needed, rather than based on a scheduled deluge cleaning and scrubbing cycles. This cleaning schedules are assumed to be fixed, i.e. there no stochastic variation in the computation of LCOMC (water) in our current analysis, and the corresponding value of LCOMC for the benchmark case is \$0.00626/kWh.

VII. CONCLUSION

Requirements of water in cleaning PV modules and CSP mirrors constitute a possible limitation on the installation of large-scale utility plants in desert and semiarid areas. Experimental studies show that a transparent EDS film can be used to laminate solar PV modules and CSP mirrors for self-cleaning function without requiring water. It is also possible to use reflective conducting electrodes for removing dust layer from solar mirrors and thus maintaining high specular reflection efficiency.

Since the output power delivered by the solar collectors depends directly on their optical efficiency, it is possible to maintain high efficiency of solar collectors in desert regions with minimum water requirements.

Optimal design, production, and operation of the EDS film need transparent conducting electrodes for their applications in PV modules and reflective conducting electrode for CSP mirrors. Availability of the electrode materials with formulations suitable for high-throughput printing processes and their outdoor durability constitute the current challenges in the EDS technology.

DRE for a wide range of particle size distribution requires optimal electrode geometry depending upon the properties of the electrode materials. SR efficiency studies showed that reflecting silver ink would work best for restoring the initial SR values of the mirrors under clean conditions.

Different methods for encapsulating Ag-electrode materials needs further investigations with respect to their durability,

electrical stability, and performance. Water-based cleaning is expensive and interruptive; EDS film technology provides a water-free cleaning method at a low operating cost. The method has a high potential for a cost-effective large-scale roll-to-roll production and for a significant reduction of O&M costs.

ACKNOWLEDGMENT

The authors would like to acknowledge the support from their partners including Corning Research & Development Corporation, Industrial Technology Research Institute, Geodrill (EDS Chile SpA), and Sandia National Laboratories and contributions from their colleagues H. Gibson, D. Crowell, F. Hao, and J. Hudelson.

REFERENCES

[1] A. Sayyah, M. N. Horenstein, and M. K. Mazumder, "Energy yield loss caused by dust deposition on photovoltaic panels," *Sol. Energy*, vol. 107, pp. 576–604, 2014.

[2] L. L. Kazmerski *et al.*, "Fundamental studies of adhesion of dust to PV module surfaces: Chemical and physical relationships at the microscale," *IEEE J. Photovolt.*, vol. 6, no. 3, pp. 719–729, May 2016.

[3] A. Sayyah, M. N. Horenstein, and M. K. Mazumder, "Mitigation of soiling losses in concentrating solar collectors," in *Proc. IEEE Photovoltaic Spec. Conf.*, Tampa, FL, USA, Jun. 2013, pp. 480–485.

[4] T. Sarver, A. Al-Qaraghuli, and L. L. Kazmerski, "A comprehensive review of the impact of dust on the use of solar energy: History, investigations, results, literature, and mitigation approaches," *Renew. Sustain. Energy Rev.*, vol. 22, pp. 698–733, 2013.

[5] D. C. Miller and S. R. Kurtz, "Durability of fresnel lenses: A review specific to the concentrating photovoltaic application," *Sol. Energy Mater. Sol. Cells*, vol. 95, no. 8, pp. 2037–2068, Aug. 2011.

[6] M. B. Sheratte, "Cleaning agents and technologies for concentrating solar collectors," Sandia Nat. Lab., Albuquerque, NM, USA, Tech. Rep. SAND79-7052, 1979.

[7] V. L. Morris, "Cleaning agents and techniques for concentrating solar collectors," *Sol. Energy Mater.*, vol. 3, nos. 1/2, pp. 35–55, 1980.

[8] G. E. Cohen, D. W. Kearney, and G. J. Kolb, "Final report on the operation and maintenance improvement for concentrating solar power plants," Sandia Nat. Lab., Albuquerque, NM, USA, Tech. Rep. SAND99-1290, 1999.

[9] A. M. Pavan, A. Mellit, and D. D. Pieri, "The effect of soiling on energy production for large-scale photovoltaic plants," *Sol. Energy*, vol. 85, no. 5, pp. 1128–1136, May 2011.

[10] M. Anderson *et al.*, "Robotic device for cleaning photovoltaic panel arrays," in *Proc. 12th Int. Conf. Climbing Walking Robots Support Technol. Mobile Mach.*, Istanbul, Turkey, Sep. 9–11, 2009, pp. 1–11.

[11] A. K. Mondal and K. Bansal, "Structural analysis of solar panel cleaning robotic arm," *Current Sci.*, vol. 108, no. 6, pp. 1047–1052, 2015.

[12] *GEKKO Solar Farm: Automated Cleaning Solution for Large Free Field Solar Power Plants*, May 22, 2017. [Online]. Available: http://bit.ly/1TVHJ3A

[13] *Heliotex: Automatic Solar Panel Cleaning Systems*, May 22, 2017. [Online]. Available: http://bit.ly/1PQfZvu

[14] S. R. Hunter *et al.*, "Low cost anti-soiling coatings for CSP collector mirrors and heliostats," *Proc. SPIE*, vol. 9175, 2014, Art. no. 91750J.

[15] G. Polizos *et al.*, "Enhanced durability transparent superhydrophobic anti-soiling coatings for CSP applications," in *Proc. ASME 8th Int. Conf. Energy Sustain.*, 2014, Art. no. V001T02A030.

[16] S. Masuda, K. Fujibayashi, K. Ishida, and H. Inaba, "Confinement and transportation of charged aerosol clouds via electric curtain," *Elect. Eng. Jpn.*, vol. 92, no. 1, pp. 43–52, 1972.

[17] R. Sims *et al.*, "Development of a transparent self-cleaning dust shield for solar panels," in *Proc. ESA-IEEE Joint Meet. Electrostatics*, Little Rock, AR, USA, Jun. 24–27, 2003, pp. 814–821.

[18] M. K. Mazumder *et al.*, "Self-cleaning transparent dust shields for protecting solar panels and other devices," *Particulate Sci. Technol.*, vol. 25, no. 1, pp. 5–20, 2007.

[19] H. Kawamoto and T. Shibata, "Electrostatic cleaning system for removal of sand from solar panels," *J. Electrostatics*, vol. 73, pp. 65–70, 2015.

[20] M. K. Mazumder *et al.*, "Self-cleaning solar mirrors using electrodynamic dust shield: Prospects and progress," in *Proc. ASME 8th Int. Conf. Energy Sustain.*, 2014, Art. no. V001T02A055.

[21] M. K. Mazumder *et al.*, "Electrodynamic removal of dust from solar mirrors and its applications in concentrated solar power (CSP) plants," in *Proc. IEEE Ind. Appl. Soc. Annu. Meeting*, Oct. 2014, pp. 1–7.

[22] A. Sayyah, M. N. Horenstein, and M. K. Mazumder, "A comprehensive analysis of the electric field distribution in an electrodynamic screen," *J. Electrostatics*, vol. 76, pp. 115–126, 2015.

[23] N. Joglekar, E. Guzelsu, M. K. Mazumder, A. Botts, and C. Ho, "A levelized cost metric for EDS-based cleaning of mirrors in CSP power plants," in *Proc. ASME 8th Int. Conf. Energy Sustain.*, 2014, Art. no. V001T02A026.

[24] S. Garner, S. Glaesemann, and X. Li, "Ultra-slim flexible glass for roll-to-roll electronic device fabrication," *Appl. Phys. A*, vol. 116, no. 2, pp. 403–407, 2014.

[25] *3M 8146-2 Optically Clear Adhesive (OCA)*, May 22, 2017. [Online]. Available: http://bit.ly/2r5aukJ

[26] M. N. Horenstein, M. K. Mazumder, and R. C. Sumner, "Predicting particle trajectories on an electrodynamic screen—Theory and experiment," *J. Electrostatics*, vol. 71, no. 3, pp. 185–188, 2013.

[27] M. K. Mazumder *et al.*, "Mitigation of dust impacts on solar collectors by water-free cleaning with transparent electrodynamic films: Progress and challenges," in *Proc. IEEE 43th Photovoltaic Spec. Conf.*, Portland, OR, USA, 2016, pp. 2052–2057.

[28] *JSC Mars-1A: A Martian Soil Simulant*, May 22, 2017. [Online]. Available: http://bit.ly/2nG6fto

[29] J. A. Cross, *Electrostatics: Principles, Problems and Applications*. Bristol, U.K.: Adam Hilger, 1987.

[30] M. N. Horenstein *et al.*, "Modeling of trajectories in an electrodynamic screen for obtaining maximum particle removal efficiency," *IEEE Trans. Ind. Appl.*, vol. 49, no. 2, pp. 707–713, Mar./Apr. 2013.

[31] A. Sayyah, M. N. Horenstein, and M. K. Mazumder, "Performance restoration of dusty photovoltaic modules using electrodynamic screen," in *Proc. IEEE Photovoltaic Spec. Conf.*, Jun. 2015, pp. 1–3.

[32] A. Sayyah, M. N. Horenstein, M. K. Mazumder, and G. Ahmadi, "Electrostatic force distribution on an electrodynamic screen," *J. Electrostatics*, vol. 81, pp. 24–36, 2016.

[33] A. Sayyah, R. S. Eriksen, M. N. Horenstein, and M. K. Mazumder, "Performance analysis of electrodynamic screens based on residual particle size distribution," *IEEE J. Photovolt.*, vol. 7, no. 1, pp. 221–229, Jan. 2017.

[34] S. Aggarwal, M. F. van Hest, J. D. Perkins, and D. S. Ginley, "Improving mechanical stability and electrical properties of silver nanowire films with a zinc tin oxide overcoat," in *Proc. IEEE Photovoltaic Spec. Conf.*, 2014, pp. 1022–1026.

[35] M. K. Mazumder *et al.*, "Development of transparent electrodynamic screens on ultrathin flexible glass film substrates for retrofitting solar panels and mirrors for self-cleaning function," *MRS Adv.*, vol. 1, no. 15, pp. 1003–1012, 2016.

[36] M. W. Knight, J. van de Groep, P. C. P. Bronsveld, W. C. Sinke, and A. Polman, "Highly conductive Ag nanowire hybrid electrodes improve silicon heterojunction solar cells," in *Proc. IEEE Photovoltaic Spec. Conf.*, Portland, OR, USA, 2016, pp. 1130–1134.

[37] *FRED Optical Engineering Software*, May 22, 2017. [Online]. Available: http://photonengr.com/software/

[38] *Henkel Adhesives*, May 22, 2017. [Online]. Available: http://bit.ly/2elUWlo

[39] A. Sayyah, "Mitigation of soiling losses in solar collectors: Removal of surface-adhered dust particles using an electrodynamic screen," Ph.D. dissertation, Dept. Elect. Comput. Eng., Boston Univ., Boston, MA, USA, 2015.

[40] A. Sayyah, D. R. Crowell, A. Raychowdhury, M. N. Horenstein, and M. K. Mazumder, "An experimental study on the characterization of electric charge in electrostatic dust removal," *J. Electrostatics*, vol. 87, pp. 173–179, 2017.

[41] S. Alqatari *et al.*, "Cost and performance comparative model for dust mitigation technologies for solar PV in Saudi Arabia," *J. Environm. Sci.*, 2015. vol. 4. [Online]. Available: http://environment.scientific-journal.com/toc/volume-4.html

Malay K. Mazumder (LF'12) received the B.Sc. (Hons.) degree in physics and the M.Sc. degree in electronics from the University of Calcutta, Kolkata, India, in 1956 and 1959, respectively, and the Ph.D. degree in instrumental sciences from the University of Arkansas at Little Rock, Little Rock, AR, USA, in 1971.

He is currently a Research Professor with the Department of Electrical and Computer Engineering, Boston University, Boston, MA, USA, where he has been since 2009. He was with the Department of Electrical Engineering, Massachusetts Institute of Technology, Cambridge, MA, as a Visiting Professor, before joining Boston University. He is involved in teaching solar energy systems and in research related to light transmission and reflection processes in photovoltaic and CSP systems. He served as a University Professor of applied science and was involved in teaching and research in the field of electrostatic engineering processes, electrodynamic systems, particle technology, and material engineering, with the University of Arkansas at Little Rock. He has authored or coauthored more than 100 publications in the fields of electrodynamic systems, material sciences, and electrostatic engineering. He has written a number of book chapters and holds three patents.

Prof. Mazumder serves as the Co-Editor-in-Chief of *Particulate Science and Technology: An International Journal*. He is also active in community service. He served as a Commissioner of the Arkansas Martin Luther King Jr. Commission under an appointment by the then-Governor M. Huckabee.

Mark N. Horenstein (LF'17) received the M.S. degree from the University of California, Berkeley, CA, USA, in 1975, and the Ph.D. and S.B. degrees from Massachusetts Institute of Technology, Cambridge, MA, USA, in 1978 and 1973, respectively, all in electrical engineering.

He is a Professor with the Department of Electrical and Computer Engineering, Boston University, Boston, MA, where he has been on the faculty since 1979. He has worked in numerous areas related to electrostatics, including instrumentation and measurement, discharges, applications and theory of corona, microelectromechanical system devices, charge and voltage sensors, dust particle dynamics, electrostatic dust removal, and high-voltage insulation. Prior to coming to Boston University, he was with Spire Corporation in the area of high-voltage pulsed power. He is the author of two text books: one on electronics and the other on the subject of engineering design. He is the author of two book chapters and has authored or coauthored more than 50 journal and conference papers. He holds five U.S. patents in the areas related to electrostatics.

Prof. Horenstein was named International Fellow by the European Working Party-Static Electricity in Industry in 2013. He is a member and the past President of the Electrostatics Society of America and was the Editor-in-Chief Emeritus of the *Journal of Electrostatics* from 2001 to 2015.

Nitin R. Joglekar (M'88) received the Bachelor's degree in engineering (with honors) from the Indian Institute of Technology, Kharagpur, India, the Master's degrees in engineering from Massachusetts Institute of Technology (MIT), Cambridge, MA, USA, and Memorial University of Newfoundland, St. John's, NL, Canada, and the Ph.D. degree in management science from the MIT Sloan School of Management, Cambridge, 1977, 1984, 1987, and 1997, respectively.

He is an Associate Professor of operations and technology management with the School of Management, Boston University, Boston, MA. Prior to his academic career, he worked in computer and ship building/offshore oil industries. He was a Founder of a venture capital backed software firm. He advises entrepreneurial and established firms in their initiatives for achieving business growth and profitability. He is now serving as a Department Editor of the IEEE TRANSACTION OF ENGINEERING MANAGEMENT.

Arash Sayyah received the B.Sc. degree from Shahid Beheshti University, Tehran, Iran, and the M.S. degree from the University of Illinois at Urbana-Champaign (UIUC), Urbana, IL, USA, in June 2007 and May 2010, respectively, both in electrical engineering, and the Ph.D. degree in electrical and computer engineering from Boston University (BU), Boston, MA, USA, in September 2015.

From October 2015 to October 2016, he was a Postdoctoral Scholar with the Applied Electromagnetics Laboratory, BU. As an Undergraduate Research Assistant, he worked on the minimization of current harmonic losses in high-power electrical machines. For his M.S. thesis with UIUC, he worked on the development of a biomechanical energy harvesting device. He is the author of two book chapters and has authored or coauthored more than 25 journal and conference papers. His research with BU focused on the mitigation of soiling losses in solar collectors using electrodynamic screens (EDS). He contributed to the EDS development project by conducting different theoretical studies, analytical calculations, and numerical simulations, as well as a number of experimental studies in order to improve the dust removal efficiency of EDS. Since November 2016, he has been a Postdoctoral Associate with the Department of Chemical Engineering, Massachusetts Institute of Technology, Cambridge, MA, USA, working on modeling and simulation of electrostatic projection of grains and powders for industrial manufacturing processes.

Dr. Sayyah was a Finalist in the Best Student Paper Award Competition and received the Graduate Student Assistant Award at the IEEE Photovoltaic Specialists Conference in 2015.

Jeremy W. Stark received the Bachelor's degrees in physics and systems engineering from the University of Arkansas at Little Rock, Little Rock, AR, USA, in 2009, where he worked in the development of laser Doppler velocimeter based particle characterization systems, and optimization of optical systems for alternative energy research.

While completing his graduate work in electrical engineering with Boston University (Master's and Doctorate), Boston, MA, USA, he worked as a Lab Instructor and Researcher with the Applied Electromagnetics Laboratory, where he led the development of self-cleaning solar panel systems. He is currently an Electronics Engineer with MagCanica, San Diego, CA, USA, leveraging his breadth and depth of technical knowledge to help optimize the design of a variety of MagCanica signal conditioning and processing circuits.

Annie A. R. Bernard received the B.Eng. degree from Anna University, Chennai, India, and the M.S. degree from Boston University (BU), Brookline, MA, USA, in May 2014 and September 2016, respectively, both in electrical and computer engineering. She is currently working toward the Ph.D. degree with the Applied Electromagnetics Laboratory, Department of Electrical and Computer Engineering, BU.

During her graduate career, she was an active committee member of the BU Energy Club. Her graduate research assistantship included work on reflective electrode materials, transparent conductive inks, and charging mechanism of particles in an electric field. She works on fabrication and developing the electrodynamic screen from a laboratory technology to a commercial product.

Sean M. Garner received the B.Eng. degree in engineering physics (applied laser and optics) from Stevens Institute of Technology, Hoboken, NJ, USA, in 1993, and the Ph.D. degree in electrical engineering (electrophysics) from the University of Southern California, Los Angeles, CA, USA, in 1998.

He is a Senior Research Associate with Corning's Science and Technology Center, Corning, NY, USA. Since 1998, he has been working in the area of material processing and device prototyping.

Julius E. Yellowhair received the B.S. degree in optical engineering from the University of Arizona, Tucson, AZ, USA, the M.S. degree in electrical engineering from the University of New Mexico, Albuquerque, NM, USA, and the M.S. and Ph.D. degrees in optical sciences from the University of Arizona, in 1996, 2002, 2005, and 2007, respectively.

He is a senior staff member with Sandia National Laboratories, Albuquerque, working in the area of solar energy technologies. His research interests include solar collector modeling, design and evaluation, and optical metrology development, including hardware and software tools, for use in solar technologies.

Hung Yi Lin received the Ph.D. degree in material science and engineering from National Tsing Hua University, Hsinchu, Taiwan, in 2003.

He is currently the R&D Deputy Director with the Advanced Manufacturing Technology Division, Mechanical and Systems Research Laboratories/Industrial Technology Research Institute, Hsinchu, Taiwan. His research interests are mainly focused on ultraprecision machining technology, nanofabrication and nanoimprint technology, and nanodevice and microelectromechanical system process technology.

Ryan S. Eriksen received the B.A. degree in physics in May 2010 from Boston University (BU), Boston, MA, USA, where he was accepted into the graduate program with a Deans Fellowship in 2010, and the M.S. and Ph.D. degrees in materials science and engineering in September 2015.

During his graduate career, he was the President of the BU Energy Club during 2012–2013 and the BU ASM Chapter during 2013–2014, where he was active in science outreach for high school students. His graduate research included work on fuel cell interconnects, thermoelectrics, and chemical sensors, for which he did an internship at Idaho National Laboratory in 2011. He is currently a Postdoctoral Associate with the Applied Electromagnetics Laboratory, Department of Electrical and Computer Engineering, BU. He serves as the Project and Laboratory Manager, working on developing the electrodynamic screen from a laboratory technology to a commercial product.

Alecia C. Griffin is currently an undergraduate student in the Department of Electrical and Computer Engineering at Boston University, Boston, MA, USA. She will graduate in 2019 with the B.S. degree in electrical engineering. She is a sophomore in electrical engineering with an energy technologies concentration. She is a Research Assistant with the Solar Energy Research Laboratory, funded by the Presidential Scholarship and by Boston University's Undergraduate Research Opportunities Program. She works on the testing of electrodynamic screens. She is also a member and mentor with the Boston University's Undergraduate Women in Science and Engineering program. She aims to further pursue her interests of sustainability and software engineering in the field of renewable energy.

Yujie Gao received the B.S. degree in materials science and engineering with a concentration in polymer materials engineering and a minor in business English from Jilin University, Changchun, China, in 2014. She is currently working toward the M.S. degree in materials science with a concentration in materials for energy and environment with Boston University, Boston, MA, USA.

During her Bachelor's studies, she conducted a research on the flame retardant performance of basalt/jute/polypropylene composites. She is conducting research on self-cleaning electrodynamic screens to be used for solar cells. Her research interests include solar energy, semiconductor materials, nanoelectronics devices and systems, and polymer materials.

Ricci La Centra received the B.A. degree in writing from Emerson College, Boston, MA, USA, arriving at engineering from a non-traditional background, and used the skills developed there in a copyediting position with the Federal Aviation Agency. He is working toward the Master's degree in materials science with Boston University, Brookline, MA.

As an engineering student, his research interests include materials that support energy conservation. He is currently researching self-cleaning electrodynamic screens to boost solar cell functions.

Alexis H. Lloyd received the Bachelor's degree in chemistry from Barnard College, New York, NY, USA, in 2012. She is working toward the Master's in science degree in materials science and engineering with a focus in materials for energy and environment with Boston University (BU), Boston, MA, USA.

She is currently conducting research on electrodynamic screens with the Applied Electromagnetics Laboratory, BU. She is enthusiastic about the great potential of advances in solar and green technologies.